

Performance of OFDM/TDM with MMSE-FDE Using Pilot-assisted Channel Estimation

Haris Gacanin and Fumiyuki Adachi

Department of Electrical and Communication Engineering, Graduate School of Engineering, Tohoku University
6-6-05 Aza-Aoba, Aramaki, Aoba-ku, Sendai 980-8579, Japan
E-mail: haris@mobile.ecei.tohoku.ac.jp

Abstract—We present, in this paper, pilot-assisted channel estimation (CE) for orthogonal frequency division multiplexing combined with time division multiplexing (OFDM/TDM) using minimum mean square error frequency-domain equalization (MMSE-FDE) over a nonlinear and frequency-selective fading channel. Joint use of time-domain filtering to increase the signal-to-noise ratio (SNR) of pilot signal and frequency-domain interpolation for OFDM/TDM is presented. The simulation results show that OFDM/TDM with proposed pilot-assisted CE provides a better performance than OFDM since the peak-to-average power ratio (PAPR) problem can be reduced.

I. INTRODUCTION

Orthogonal frequency division multiplexing (OFDM) signals have a problem with high peak-to-average power ratio (PAPR). Due to high PAPR, after nonlinear high-power amplifier (HPA), the OFDM signals will be distorted, which as a consequence may lead to severe degradation of bit error rate (BER) performance. Recently [1], we proposed OFDM combined with time division multiplexing (OFDM/TDM) to overcome the high PAPR of OFDM. However, OFDM/TDM cannot completely eliminate the PAPR problem [2]. In the OFDM/TDM design, the N_c -point inverse fast Fourier transform (IFFT) time window of conventional OFDM is divided into K slots (which constitutes the OFDM/TDM frame). It was shown in [1] that the BER performance of OFDM/TDM in a frequency-selective fading channel can be improved when minimum mean square error frequency-domain equalization (MMSE-FDE) is applied.

MMSE-FDE requires accurate channel estimation (CE). In a nonlinear channel (e.g., HPA), channel estimator must be carefully designed to reduce the effect of nonlinear distortions arising from the PAPR problem. Various channel estimation techniques are studied in [3]-[5], but the impact of HPA was not considered. To avoid the effect of nonlinearity, time-domain multiplexed pilot (TDM-pilot) with the constant amplitude can be used, but the tracking ability reduces [3]. A pilot symbol may be inserted onto reserved pilot subcarriers in the frequency domain (FDM-pilot) to improve the tracking ability against fast fading [4]-[6], but the pilot sequence will be distorted by HPA and this may degrade the CE accuracy. Furthermore, CE techniques in [4]-[6] cannot be directly applied to OFDM/TDM since, in the OFDM/TDM receiver, N_c -point FFT over the entire OFDM/TDM frame is applied for FDE [1]. Recently, a cyclic postfix OFDM was presented for channel estimation [7]-[9], but the computational complexity significantly increases and furthermore, the transmission efficiency reduces.

In this paper, an improved pilot-assisted CE using time-domain first-order filtering and frequency-domain

interpolation for OFDM/TDM is presented. A pilot signal is inserted into one reserved slot (i.e., pilot slot) of the OFDM/TDM frame without sacrificing the transmission efficiency. Then, time-domain first-order filtering on a slot-by-slot basis is applied to improve the signal-to-noise ratio (SNR) of pilot signal. Since all channel gains required for FDE cannot be obtained (because the number of OFDM/TDM subcarriers is $N_m=N_c/K < N_c$), frequency-domain interpolation is applied to estimate required channel gains. We consider the first-, the second- and high-order resolution frequency-domain interpolation methods.

The rest of the paper is organized as follows. Section 2 describes OFDM/TDM system model. A pilot-assisted CE is presented in Sect. 3. In Sect. 4, the BER performance is evaluated by computer simulation. Section 5 concludes the paper.

II. OFDM/TDM TRANSMISSION SYSTEM

The OFDM/TDM system model is illustrated in Fig. 1. Throughout this paper, T_c -spaced discrete time representation is used, where T_c represents FFT sampling period.

A. OFDM/TDM Signal

The signaling interval of conventional OFDM with N_c subcarriers is divided into K slots, i.e., OFDM/TDM frame. A sequence of data-modulated symbols is divided into blocks with $N_m=N_c/K$ symbols. The k -th block symbol sequence is denoted by $\{d^k(i); i=0\sim N_m-1\}$, where $d^k(i)=d(kN_m+i)$ for $k=0\sim K-2$. A pilot signal $\{p(i); i=0\sim N_m-1\}$ is inserted into the $(K-1)$ th slot (i.e., $d^{K-1}(i)=p(i)$ for $i=0\sim N_m-1$). N_m -point IFFT is applied to generate the k th OFDM signal with N_m subcarriers as

$$s^k(t) = \frac{1}{\sqrt{N_m}} \sum_{i=0}^{N_m-1} d^k(i) \exp\left(j2\pi \frac{i}{N_m} t\right) \quad (1)$$

for $t=0\sim N_m-1$. K generated OFDM signals are grouped into one frame without inserting the GI between them to generate OFDM/TDM signal (see Fig. 2). The g -th frame OFDM/TDM signal can be expressed using the equivalent lowpass representation as

$$s_g(t) = \sqrt{2} \sum_{k=0}^{K-1} s^k(t - kN_m) u(t - kN_m) \quad (2)$$

for $t=0\sim N_c-1$ and $u(t)=1(0)$ for $t=0\sim N_m-1$ (elsewhere). After insertion of an N_m -sample GI, the OFDM/TDM signal is fed to HPA, which can be approximated by soft limiter conversion characteristics as [10]

$$\hat{s}_g(t) = \begin{cases} s_g(t), & |s_g(t)| \leq \beta \\ \beta \frac{s_g(t)}{|s_g(t)|}, & \text{otherwise} \end{cases} \quad (3)$$

for $t=0 \sim N_c-1$, where β denotes the HPA saturation level. Finally, the OFDM/TDM signal is multiplied by the transmit power coefficient \sqrt{P} as shown in Fig. 1.

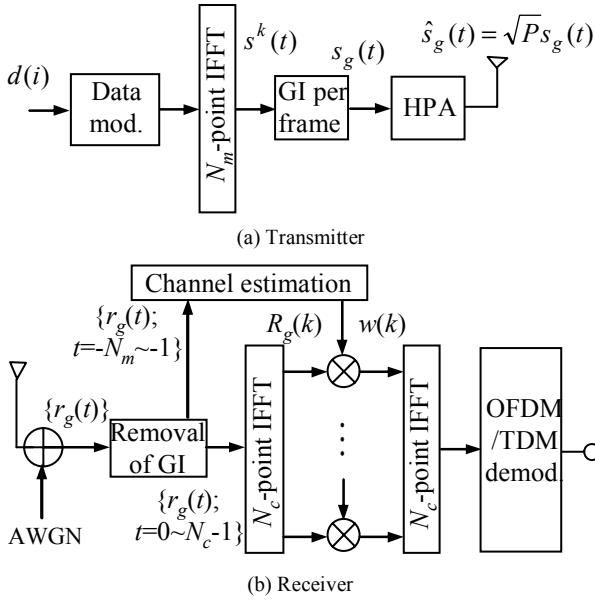


Fig. 1. OFDM/TDM transmitter/receiver structure.

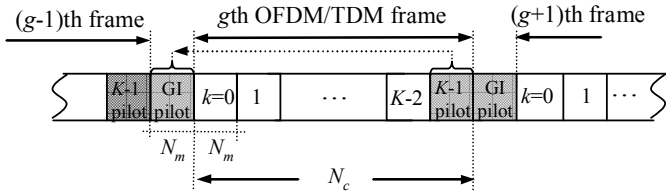


Fig. 2. OFDM/TDM frame structure.

B. FDE

The OFDM/TDM signal is transmitted over a propagation channel having the discrete-time channel impulse response $h(\tau)$, given as

$$h(\tau) = \sum_{l=0}^{L-1} h_l \delta(\tau - \tau_l), \quad (4)$$

where h_l and τ_l are the path gain and time delay of the l th path with $E[|h_l|^2] = 1/L$. The g -th frame received signal can be expressed as

$$r_g(t) = \sqrt{2P} \sum_{l=0}^{L-1} h_l \hat{s}_g(t - \tau_l) + n_g(t) \quad (5)$$

for $t=-N_m \sim N_c-1$, where $n_g(t)$ is the additive white Gaussian noise (AWGN) process with zero mean and variance $2N_0/T_c$ with N_0 being the single-sided power spectrum density. The

g th frame's GI $\{\tilde{r}_g(t); t=-N_m \sim -1\}$ (i.e., pilot signal) is stored while the received signal $\{r_g(t); t=0 \sim N_c-1\}$ is decomposed into N_c frequency components $\{R_g(n); n=0 \sim N_c-1\}$ for FDE as

$$R_g(n) = \frac{1}{N_c} \sum_{t=0}^{N_c-1} r_g(t) \exp\left(-j2\pi n \frac{t}{N_c}\right). \quad (6)$$

One-tap FDE is applied to $R_g(n)$ as [11]

$$\hat{R}_g(n) = w(n)R_g(n), \quad (7)$$

where $w(n)$ denotes the MMSE equalization weight for the n th frequency.

$w(n)$ is determined so that MSE between $\hat{R}_g(n)$ and $S_g(n)$ is minimized. After some manipulations, we can show that the theoretical MMSE weight is given by

$$w(n) = \frac{\alpha H^*(n)}{|H(n)|^2 \{1 - e^{-\beta^2}\} + 2\sigma^2}, \quad (8)$$

where $*$ denotes the complex conjugate operation. In Eq. (8), α denotes the attenuation constant of the OFDM/TDM signal due to HPA [2]; for $\beta > 7$ dB, $\alpha \rightarrow 1$ while for lower β , α can be well approximated as [10]

$$\alpha = 1 - \exp\{-\beta^2\} + \frac{\sqrt{\pi}\beta}{2} \text{erfc}\{\beta\}, \quad (9)$$

where $\text{erfc}[x] = (2/\sqrt{\pi}) \int_x^\infty \exp(-t^2) dt$ is the complementary error function. In Eq. (8), α is assumed to be known at the receiver. Note that the simple HPA model given by Eq. (3) may not be completely accurate for modeling real HPA's. Since this paper presents CE scheme, the impact of different HPA models is out of scope of this paper. We need to estimate the channel gain $H(n)$ and the noise power σ^2 . Channel estimation will be described in Sect. III.

The time-domain OFDM/TDM signal is recovered by applying N_c -point IFFT to $\{\hat{R}_g(n); n=0 \sim N_c-1\}$, and then, the demodulation of OFDM signal with N_m subcarriers is done using N_m -point FFT [1].

III. CHANNEL ESTIMATION

A pilot signal inserted into $(K-1)$ th slot is copied as a cyclic prefix into a GI at the beginning of the frame (see Fig. 2) as described in [11] for SC transmission. As illustrated in Fig. 2, the $(g-1)$ th frame's pilot slot acts as a cyclic prefix for the g th frame's GI (which is copied from the g th frame's pilot slot). Thus, the channel estimation can be performed using the g th frame's N_m -sample GI. Note that the length of GI equals to the OFDM/TDM slot length of N_m -samples. If large amplitude variations appear in the time-domain pilot signal, the pilot may be distorted due to HPA leading to poor channel estimates. On the other hand, to avoid noise enhancement in the channel estimation, it is desirable that a pilot sequence has the constant

amplitude in the frequency-domain. In this paper, Chu pilot sequence [12] is considered since its amplitude in both time-domain and frequency-domain is constant and hence, HPA will not affect CE. The Chu pilot is given by $p(i)=\cos(\pi i^2/N_c)+j\sin(\pi i^2/N_c)$ for $i=0\sim N_m-1$.

The channel gain estimate and noise power estimate to be used for FDE are denoted by $H_e(n)$ and σ_e^2 , respectively (i.e., $H(n)$ and σ^2 in Eq. (8) are replaced by $H_e(n)$ and σ_e^2 , respectively).

A. Time-domain First-order Filtering

We consider reception of the g th OFDM/TDM frame. The g th frame's GI (i.e., pilot signal) is filtered as

$$\bar{r}_g(t) = \gamma \tilde{r}_g(t) + (1-\gamma)\bar{r}_{g-1}(t) \quad (10)$$

for $t=0\sim N_m-1$, where γ is the filter coefficient with the initial condition $\bar{r}_0(t)=\tilde{r}_0(t)$. The N_m -point FFT is applied to decompose the filtered pilot signal into N_m frequency components as

$$\bar{R}_g(q) = \sum_{t=-N_m}^{-1} \bar{r}_g(t) \exp\left(-j2\pi q \frac{t}{N_m}\right), \quad (11)$$

where $q=\lfloor n/K \rfloor$ for $n=0\sim N_c-1$ is the subcarrier index and $\lfloor x \rfloor$ denotes the largest integer smaller than or equal to x . Then, the instantaneous channel gain estimate at the q th subcarrier is obtained by the reverse modulation as

$$\bar{H}_g(q) = \frac{\bar{R}_g(q)}{P(q)}, \quad (12)$$

where $P(q)$ denotes the pilot at the q th frequency.

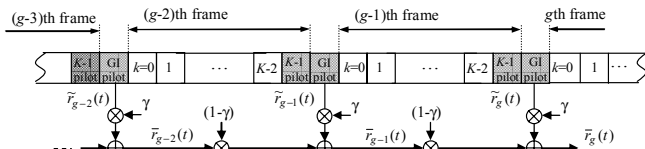


Fig. 3. First-order filtering.

B. Frequency-domain Interpolation

As shown in Fig. 4, $\{\bar{R}_g(q); q=0\sim N_m-1\}$ are located at the frequency $n=0, K, 2K, \dots, (N_m-1)K$. The separation between N_m frequencies is K while the separation between N_c frequencies is 1 and hence, interpolation [13] is necessary to obtain the channel gains for all frequencies of $n=0\sim N_c-1$. We consider the first-, the second- and high-order resolution frequency-domain interpolation methods.

(First-order interpolation) The channel gain estimate at the n th frequency using the first-order interpolation is given as

$$H_e(n) = \frac{K-i}{K} \bar{H}(\bar{n}) + \frac{i}{K} \bar{H}(\bar{n}+1), \quad (13)$$

where $i = n - K\lfloor n/K \rfloor$, $\bar{n} = \lfloor n/K \rfloor$ and $\lfloor x \rfloor$ denotes the integer larger than or equal to x .

(Second-order interpolation) The channel gain estimate by the second-order interpolation is given as

$$H_e(n) = c_0 \bar{H}(\bar{n}) + c_1 \bar{H}(\bar{n}+1) + c_2 \bar{H}(\bar{n}+2), \quad (14)$$

where

$$c_0 = \frac{(i-K)(i-2K)}{2K^2}; c_1 = \frac{i(2K-i)}{K^2}; c_2 = \frac{i(i-K)}{2K^2}. \quad (15)$$

(High-resolution interpolation) For high-resolution frequency-domain interpolation, N_m -point IFFT is performed on $\{\bar{H}(q); q=0\sim N_m-1\}$ to obtain the instantaneous channel impulse response $\{\bar{h}(t); t=0\sim N_m-1\}$ as

$$\bar{h}(t) = \frac{1}{N_m} \sum_{q=0}^{N_m-1} \bar{H}(q) \exp\left(j2\pi q \frac{t}{N_m}\right). \quad (16)$$

Then, N_c -point FFT is applied to obtain the interpolated channel gain estimates for all N_c frequency components $\{H_e(n); n=0\sim N_c-1\}$ as

$$H_e(n) = \frac{1}{N_c} \sum_{t=0}^{N_m-1} \bar{h}(t) \exp\left(-j2\pi n \frac{t}{N_c}\right). \quad (17)$$

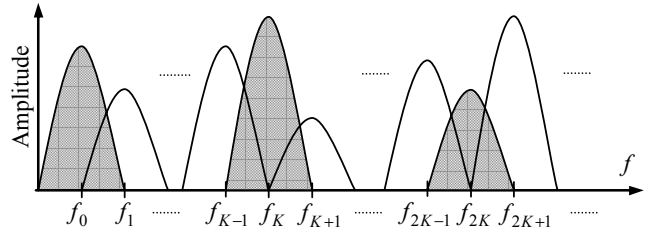


Fig. 4. Received signal spectrum.

C. Noise Power Estimation

The noise component at the q th frequency can be estimated by subtracting the received pilot component $H_e(q)P(q)$ from $\bar{R}_g(q)$ as

$$N_e(q) = \bar{R}_g(q) - H_e(q)P(q) \quad (18)$$

for $q=0\sim N_m-1$. The noise power estimate can be obtained as

$$\sigma_e^2 = \frac{1}{N_m} \sum_{n=0}^{N_m-1} |N_e(q)|^2. \quad (19)$$

IV. SIMULATION RESULTS

Simulation parameters are shown in Table 1. We assume QPSK data-modulation with $N_c=256$ and $N_m=16$. The propagation channel is $L=8$ -path frequency-selective block Rayleigh fading channel having uniform power delay profile. The path gains stay constant over one frame, but varies frame-by-frame. $f_D T_s$ is the normalized Doppler frequency with $1/T_s=1/T_c N_m$ (e.g., $f_D T_s=0.001$ corresponds to mobile terminal moving speeds of about 110 km/h for 5GHz carrier frequency and transmission data rate of 100M symbols/sec).

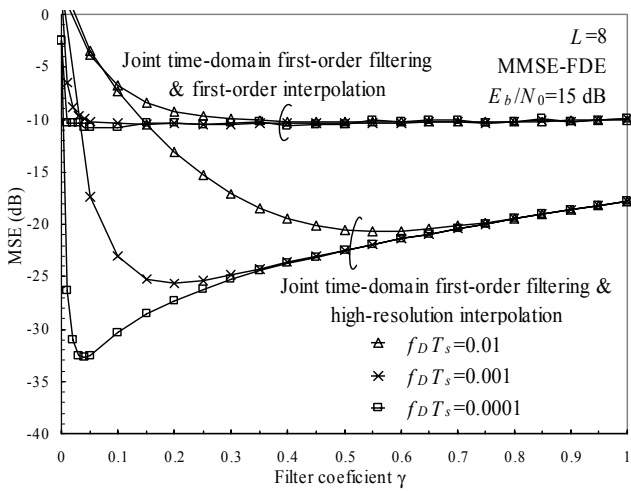


Fig. 5. MSE vs. γ .

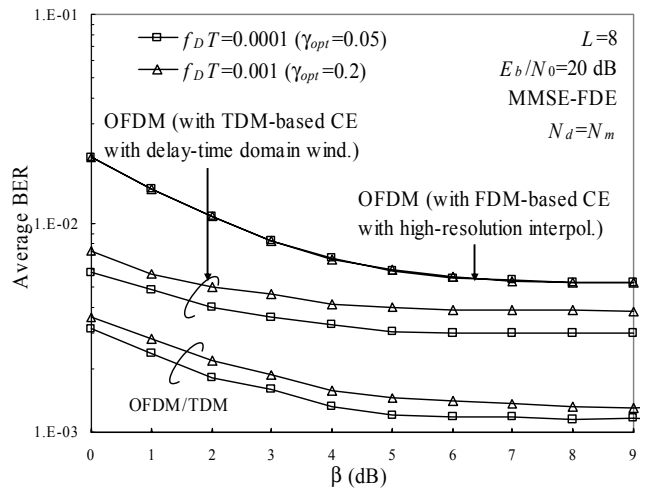


Fig. 7. BER vs. β .

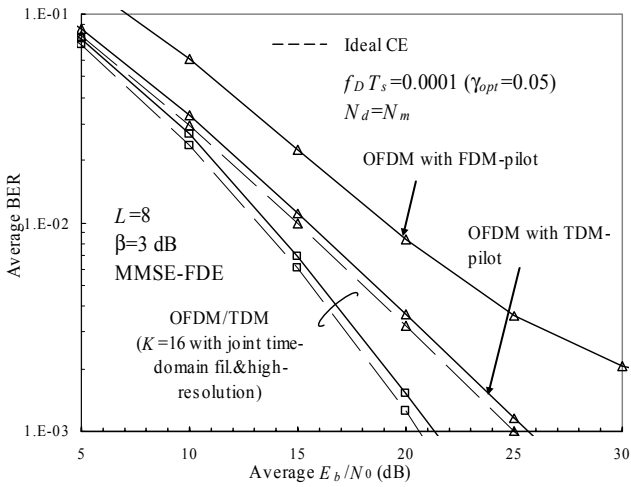


Fig. 6. BER vs. E_b/N_0 .

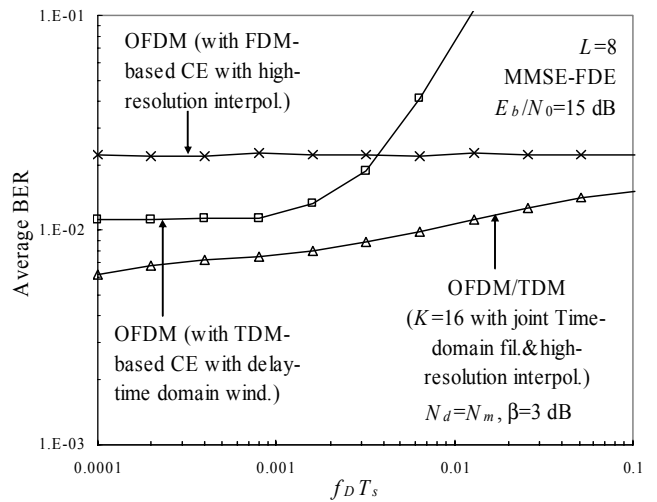


Fig. 8. BER vs. $f_D T_s$.

Throughout this section, for a fair comparison with conventional OFDM, we consider conventional OFDM system with both TDM- and FDM-pilot insertion with high-resolution frequency-domain interpolation. For CE with FDM-pilot N_m uniformly-spaced pilot subcarriers are used as presented in [4]-[6]. To eliminate the pilot distortion, CE with TDM-pilot is used, where one frame consists of OFDM pilot generated using Chu sequence followed by N_d OFDM data symbols [3]. Furthermore, an N_m -sample GI is used to keep the same transmission efficiency as our OFDM/TDM.

TABLE I. SIMULATION PARAMETERS.

Transmitter	Data modulation	QPSK
	IFFT size	$N_m=16$
No. of slots	$K=16$	
Frame length	$N_c=256$	
GI	$N_m=16$	
Channel	L -path frequency-selective Rayleigh fading	
Receiver	FFT size	$N_c=256$
	FDE	MMSE

As the time-domain filter coefficient γ decreases, the noise is reduced, but the tracking ability against fast fading tends to be lost. On the other hand, as $f_D T_s$ increases, the channel varies faster and consequently, the higher γ is required to achieve the lower MSE. Fig. 5 shows the average MSE with joint use of time-domain first-order filtering and high-resolution frequency-domain interpolation as a function of γ with $f_D T_s$ as a parameter for $E_b/N_0=15$ dB. As shown by Fig. 5, the optimum γ_{opt} for minimizing the MSE with $E_b/N_0=15$ dB, is $\gamma_{opt}=0.05$, 0.2, and 0.55 for $f_D T_s=0.0001$, 0.001 and 0.01, respectively. It is observed that the first-order interpolation provides poor performance (we confirmed by computer simulation that the second-order interpolation performs slightly better). In the following we only consider high-resolution frequency-domain interpolation.

Fig. 6 shows the average BER with the joint use of time-domain first-order filtering and high-resolution frequency-domain interpolation as a function of the E_b/N_0 for $\beta=3$ dB. The optimum γ_{opt} is used. The figure shows the good performance of the proposed CE with joint use of time-domain first-order filtering and high-resolution

frequency-domain interpolation. The E_b/N_0 degradation of OFDM/TDM in comparison to ideal CE, for $\text{BER}=10^{-3}$, is about 0.8 dB when $f_D T_s=0.0001$. It can be seen from the figure that OFDM with FDM-pilot achieves a poor performance because of interpolation error and the signal distortion due to HPA. In particular, $\text{BER}=10^{-3}$ cannot be achieved. However, OFDM with TDM-pilot achieves much better BER performance since the effect of HPA nonlinearity can be avoided; when $f_D T_s=0.0001$ the E_b/N_0 degradation for $\text{BER}=10^{-3}$ from ideal CE case is about 0.8 dB. However, a problem of CE with TDM-pilot is the increased tracking error in a fast fading environment (see Fig. 8). The OFDM/TDM with the proposed CE using jointly time-domain first-order filtering and high-resolution frequency-domain interpolation achieves a much better BER performance than OFDM; when $f_D T$ is 0.0001 the required E_b/N_0 for $\text{BER}=10^{-2}$, reduces by about 5.5 and 2 dB in comparison with OFDM using FDM- and TDM-pilot insertion, respectively.

Fig. 7 shows the average BER performance of pilot-assisted CE with time-domain first-order filtering and high-resolution frequency-domain interpolation as a function of β for the $E_b/N_0=20$ dB with $f_D T_s$ as a parameter. The optimum γ_{opt} is used for each $f_D T_s$. It can be seen from the figure that the BER performance degradation of OFDM/TDM with $K=16$ for $\beta>4$ dB is negligible. On the other hand, the BER of OFDM degrades until about $\beta=6$ dB. The OFDM/TDM provides a better performance with lower β than OFDM since the PAPR problem with OFDM/TDM is reduced.

The normalized Doppler frequency $f_D T_s$ is an important parameter that affects the BER performance. To show the advantage of OFDM/TDM over OFDM on a fast fading, Fig. 8 plots the BER performance of pilot-assisted CE with the joint use of time-domain first-order filtering and high-resolution frequency-domain interpolation as a function of the $f_D T_s$ for $E_b/N_0=15$ dB. For comparison we also plot curves for OFDM with CE using both FDM- and TDM-pilots. The optimum γ_{opt} is used for each $f_D T_s$ value. When $f_D T_s<0.003$, OFDM with TDM-pilot achieves lower BER than FDM-pilot since pilot distortion due to HPA nonlinearity can be avoided; but, as $f_D T_s$ increases, the tracking ability tends to be lost and the performance severely degrades. However, OFDM/TDM gives a lower BER than conventional OFDM due to frequency diversity gain and a lower PAPR leading to less performance degradation by HPA.

V. CONCLUSIONS

In this paper, pilot-assisted CE which jointly uses time-domain first-order filtering (to increase the SNR of pilot signal) and frequency-domain interpolation was proposed for OFDM/TDM with MMSE-FDE in a nonlinear and frequency-selective fading channel. It was shown by the computer simulation that the joint use of time-domain first-order filtering and high-resolution frequency-domain interpolation provides a very good tracking ability against fast

fading and that OFDM/TDM with proposed pilot-assisted CE always achieves better BER performance than OFDM.

REFERENCES

- [1] H. Gacanin, S. Takaoka and F. Adachi, "Bit error rate analysis of OFDM/TDM with frequency-domain equalization," in Proc. 62th IEEE VTC, September 25-28, 2005, Dallas, Texas, USA.
- [2] H. Gacanin and F. Adachi, "Reduction of Amplitude Clipping Level with OFDM/TDM," in Proc. 64th IEEE VTC, Montreal, Canada, Sep. 2006.
- [3] H. Gacanin, S. Takaoka and F. Adachi, "Pilot-assisted Channel Estimation for OFDM/TDM with Frequency-domain Equalization," in Proc. 62th IEEE VTC, September 25-28, 2005, Dallas, Texas, USA.
- [4] R. Negi and J. Cioffi, "Pilot tone selection for channel estimation in a mobile OFDM system," IEEE Trans. Consumer Electron., vol. 44, no. 3, Aug. 1998.
- [5] M. Hsieh and C. Wei, "Channel estimation for OFDM systems based on comb-type pilot arrangement in frequency selective fading channels," IEEE Trans. Consumer Electron., vol. 44, no. 1, Feb. 1998.
- [6] S. Coleri, M. Ergen, A. Puri, and A. Bahai, "Channel estimation techniques based on pilot arrangement in OFDM systems," IEEE Trans. Broad., Vol. 48, No. 3, pp. 362-370, Sept. 2002.
- [7] M. Much, M. de Courville, M. Debbah and P. Duhamel, "A pseudo random postfix OFDM modulator and inherent channel estimation techniques," in Proc. Globecom., vol. 4, pp. 2380-2384, Dec. 2003.
- [8] M. Much, M. de Courville, M. Debbah and P. Duhamel, "Iterative interference suppression for pseudo random postfix OFDM channel estimation," in Proc. ICASSP, vol. 3, pp. 765-768, Mar. 2005.
- [9] J. Kim, S. Lee and J. Seo, "Synchronization and channel estimation in cyclic prefix based OFDM system," in Proc. IEEE 63th VTC, Melbourne, Australia, May 2006.
- [10] J. Tellado, L. M. C. Hoo and J. M. Cioffi, "Maximum-likelihood detection of nonlinearly distorted multicarrier symbols by iterative decoding," IEEE Trans. on Commun., Vol. 51, No. 2, Feb. 2003.
- [11] D. Falconer, S.L. Ariyavisitakul, A. Benyamin-Seeyar, and B. Eidson, "Frequency-domain equalization for single-carrier broadband wireless systems," IEEE Commun. Mag., Vol. 40, pp.58-66, April 2002.
- [12] D. C. Chu, "Polyphase codes with good periodic correlation properties," IEEE Trans. on Inf. Theory, July 1972, pp. 531-532.
- [13] G. A. Korn and T. M. Korn, *Mathematical Handbook for Scientists and Engineers*, 2nd ed. New York: Dover Publications, 2000.